Fatima Zohra Khelif [*], *Mustapha Helmaoui, Fayçal Bouzit, Hanaa Derraz, Atika Bencherif, Mohamed Bouzit*

NUMERICAL STUDY OF DAM-BREAK ON MULTI-POROUS BREAKWATER

NUMERIČKA ANALIZA PUCANJA BRANE NA VIŠESTRUKO POROZNU KONSTRUKCIJU ZA RAZBIJANJE TALASA

Originalni naučni rad / Original scientific paper
UDK /UDC:

Rad primljen / Paper received: 9.05.2023

Adresa autora / Author's address:
LSIM, Faculty of Mechanical Engineering, University of Science and Technology of Oran, Mohamed Boudiaf, El Mnaouar, Oran, Algeria
[*]email: fatimazohra.khelif@univ-usto.dz

Keywords
- wave breaker
- VOF method
- dam-break
- porous breakwater
- wave interaction

Ključne reči
- razbijanje talasa
- VOF metoda
- pucanje brane
- porozna konstrukcija za razbijanje talasa
- interakcija talasa

Abstract

Wave breakers are one of the means used to protect and prevent the coastline, infrastructure, and human life from the risks of waves. With this in mind, a numerical study has been carried out of a breaking wave caused by a water dam breaking through a rectangular wave breaker composed of four successive porous media arranged in order of increasing Darcy number (reflecting the porosity) and then in decreasing order. The objective of the paper is to study numerically the profile of the free surface of water, the pressure, and pressure on the outer wall of the model, as well as the velocity field. The two-phase flow (VOF) model has been used to describe the deformation of the free surface. The equations are presented and solved numerically using the finite element method. According to the obtained numerical results, for the wave breaker with decreasing porosity panels, the wave caused by the break of the dam reaches the outer wall earlier, so that the equilibrium is reached earlier than the wave passing through the wave breaker with decreasing porosity and that the velocities are relatively higher. For the wave breaker with decreasing porosity, the pressures exerted on the outer wall by the wave are more important.

Izvod

Konstrukcije za razbijanje talasa su jedan od postupaka koji se koriste za zaštitu i prevenciju od uticaja talasa na obale, infrastrukturu i za zaštitu ljudi. Stoga je izvedena numerička analiza razbijanja talasa vodenom branom, primenom pravougaone konstrukcije za razbijanje talasa koja se sastoji iz četiri sukcesivne porozne sredine, raspoređene u smeru porasta Darsijevog broja (mere poroznosti), a zatim u smeru opadanja. Cilj rada je izučavanje numeričkog profila slobodne vodene površine, pritiska, pritiska na spoljni zid modela, kao i brzinsko polje strujanja. Model dvofaznog strujanja (VOF) je primenjen za opisivanje deformacije slobodne površine. Predstavljene su jednačine i dato je njihovo numeričko rešavanje metodom konačnih elemenata. Prema dobijenim numeričkim rezultatima, u konstrukciji za razbijanje talasa sa panelima opadajuće poroznosti, talas koji nastaje pucanjem brane stiže do spoljnjeg zida ranije, tako da se ravnoteža uspostavlja ranije u odnosu na talas koji prolazi kroz konstrukciju za razbijanje sa opadajućom poroznošću, a brzine su relativno veće. Mnogo su važnije vrednosti pritisaka talasa na spoljni zid u konstrukcijama za razbijanje talasa sa opadajućom poroznošću.

INTRODUCTION

The coastline is a particular territory which is currently threatened. The establishment of a knowledge base on wave phenomena in order to cope with their behaviour and thus define more efficient protection methods to avoid catastrophic consequences up to the prevention of human losses as well as damages to infrastructures and environment. For this purpose, many researchers have shown a particular interest. Peng et al. /1/ investigate numerically the impact of a dam-break induced flood on a structure and found that at the cross-section the water profile surface downstream and upstream the structure and the surface velocity distribution are not completely the same, they also observed that the pressure can reach 1.5 to 3 times the pressure after first impact when they simulate a dam-break flood on a solitary structure in the downstream location. Kai Cheng Hu /2/ in order to describe the hydrodynamics of the dam-break interaction with porous structures, a series of three-dimensional macroscopic governing equations have been derived that integrate the spatially averaged resistance force, and have incorporated the turbulence model and algorithm of the moving solids to observe the behaviour of the waves in the porous medium, and found that the latter reduces the normal impact force, and that the net force and maximum net forces are reduced as the distance from the dam increases. Reza Marsooli and Weiming Wu /3/ developed a three-dimensional model of dam failure flows on an irregular bed by solving the RANS equations using an explicit finite volume. They focused on the dynamic pressure load of dam-break wave on structures and the vertical distribution of flow properties. Their results reveal that the vertical velocity can be up to 81 % of the horizontal velocity and the pressure may not be hydrostatic at the initial stages of dam-break flow. Alibek Issakhov and Aliya Borsikbayeva /4/ in their numerical study took into account the comportment of an incompressible fluid, sediments, and solid particles at the time of a dam-break by

inserting a complex protection system by installing cylindrical columns at several levels which led to a slowing down of the propagation of the breaking wave thus giving time for evacuation. Arun Kamath et al. /5/ investigated the interaction of a wave with a cylinder for several wave elevations and impact scenarios at different cylinder positions with an open source CFD model. Hyoungsu Park et al. /6/ in order to validate the CFD model and compare the ANSYS -FLUENT® and IHFOAM® models they have simulated three regular wave conditions which generate non-breaking, breaking, and broken wave impact on a structure by introducing the residual impulse to quantitatively evaluate the variation of the force and pressure time series. Hongyue Sun et al. /7/ studied numerically the effect of air compressibility in different modes of breaking wave using a CIP (Constrained Interpolation Profile) method to discretize Navier-Stokes equations. They found that that the impact pressure oscillation is synchronic with the compression and expansion of the trapped air pocket and the oscillation frequency is relative to the air pocket size. For air-water mixture impact, the pressure oscillation can be more intense.

Several experimental studies have been conducted by M. Salih Kirkgöz /8-11/. In the first, he has tested the breaking oscillating waves impact pressure and deformations on a vertical wall with a 1/10 foreshore slope. The results showed that consideration should be given to low magnitude impact forces that last longer because they cause more deformation. Afterwards, he investigated the impact pressure of a breaking wave on a sloping or vertical wall and found that pressures are greater on a sloping than on a vertical wall. Next, he conducted an experimental study to measure the impact pressure and deformation caused by different depths of a breaking wave on a vertical, inclined 10° and 30° wall with a 1/10 foreshore slope. In 1995, he examined the impact pressure from wave breaking (early, late, and perfect breaking) directly on the vertical and inclined coastal structures (various inclinations).

Masataro Hattori et al. /12/, in order to improve their comprehension of the impact pressure due to waves breaking against a vertical wall, they used high speed video images of waves at the time of collision to measure it. They focused on the following collision conditions: flip-through, collision of vertical wave front, and collision of the plunging wave. R. Manjula et al. /13/ made an experimental investigation regarding the effect of breaking waves of different intensities on a thin vertical cylinder by measuring the pressure and acceleration. In W.Y. Sun et al. /14/, in order to study the performance of a submerged porous breakwater, an open-source flow solver (REEF3D) was used to solve the equations of incompressible two-phase flow. Several factors were considered to investigate the hydrodynamic characteristics of coastal bridge decks. The study showed that submerged porous wave breakers reduce hydrodynamic loads and should be advantageous for bridge design. Enjin Zhao et al. /15/ numerically investigated the effect of a breaking solitary wave on a semi-circular breakwater in porous medium based on the immersed boundary method (IB) where they found that, increasing the gravel size decreases the wave height and the horizontal hydrodynamic force while the vertical hydrodynamic force increases. Tandem wave breakers have more impact on wave propagation than single wave breakers. After validation of the SPH porous model Bing Ren et al. /16/ modelled wave motions and turbulent flows through porous structures to study the interaction of waves with submerged and emerged rubble-mound breakers in two-layer porous media. Good agreements are obtained between the computed results and experimental data. Dongsheng Qiao et al. /17/ have analysed with a numerical CFD model using a macroscopic approach the effect of wave characteristics and porosity on horizontal waves, reflection coefficient, and transmission, and have therefore demonstrated the reliability of their model. In Santanu Koley et al. /18/ three different types of breakwaters are considered to show the effect of wave height and the height of RMOB's on wave reflection, wave transmission, and wave energy dissipation. Wenan Wua et al. /19/ investigated the hydromechanics of saturated and semi-saturated porous soil-rock mixture (SRM) using the numerical manifold method (NMM) on the basis of fully coupled dynamics. Hongjie Wen et al. /20/ study the wave interaction with a detached breakwater, parallel to the coast, composed of two layers of porous media. The predicted 3D flow field inside and outside the permeable breakwater and the spatial distributions of the wave breaking induced current are analysed and discussed. In order to study the fluid-porous structure interaction, Ebrahim Jafari et al. /21/ used a new formulation of an Eulerian FVM-VOF method to model the flow in the fluid and in the porous medium, while for the simulation of the deformations of the breakwater, a porosity adjustment as well as a DEM Lagrangian method were used. They found that this model can provide an accurate simulation of the free surface, the flow through the porous medium and deformations of the breakwater. In order to confirm their numerical methods, Dan Hu et al. /22/, Jie-min Zhan et al. /23/ simulated a wave tank with Navier-Stocks equations and the VOF method, where they used the energy dissipation property of porous media. With a hybrid open source Porous Inter Foam software based on the Darcy-Brinkman multiphase approach, using a unique set of partial differential equations, Francisco J. Carrillo et al. /24/ simulated a two-phase flow of both solids-free and porous regions. This proposed model tends toward the Navier-Stokes volume of fluid approach in the solids-free regions and toward multiphase Darcy equations in porous regions. The work of H. Grzybowski and R. Mosdorf /25/ consisted in the numerical study of a two-phase flow in a mini channel where the level-set method was used for capturing the liquid-gas interface. For solving Navier-Stocks equations, Comsol Multiphysics® on a two-dimensional mesh has been implemented.

This paper deals with wave propagation due to dam failure in the presence of four consecutive rectangular breakwaters of different porosity and consists of five sections. In the introduction, previous research carried out in the field is reviewed. In section 2, fundamental equations governing the problem and boundary conditions are mentioned. In section 3, the proposed physical geometry, validation results, and results found in literature are presented. In section 4, computational simulation results show effects of vertically increasing and decreasing porosity in a rectangular breakwater.

Finally, section 5 represents an overall conclusion summarizing the main results obtained in the paper.

FUNDAMENTAL RELATIONS

Governing equations

The propagation of the breaking wave is governed by the equations describing the mass and momentum balance as well as the volume fraction of the two phases. The two-phase flow (VOF) model has been used to describe the deformation of the free surface. The liquid part (water) corresponds to volume fraction φ = 0, whereas the gas phase (air) corresponds to the volume fraction of φ = 1.

The equations that are solved by the VOF model are as follows:

Continuity equation:

$$\frac{\partial u}{\partial x}+\frac{\partial v}{\partial y}=0 \quad . \tag{1}$$

Momentum equation:

$$\rho\left(\frac{\partial u}{\partial t}+u\frac{\partial u}{\partial x}+v\frac{\partial u}{\partial y}\right)=-\frac{\partial p}{\partial x}+\mu\left(\frac{\partial^2 u}{\partial x^2}+\frac{\partial^2 u}{\partial y^2}\right)-\frac{\mu}{K}u \quad , \tag{2}$$

$$\rho\left(\frac{\partial u}{\partial t}+u\frac{\partial v}{\partial x}+v\frac{\partial v}{\partial y}\right)=-\frac{\partial p}{\partial y}+\mu\left(\frac{\partial^2 v}{\partial x^2}+\frac{\partial^2 v}{\partial y^2}\right)-\rho g-\frac{\mu}{K}v \quad . \tag{3}$$

The medium is described by volume fraction φ of one of the phases without exchange between phases. The value of φ in each computational cell is a problem variable that is advected with the velocity $V(u, v)$.

Convection equation:

$$\frac{\partial \varphi}{\partial t}+u\frac{\partial \varphi}{\partial x}+v\frac{\partial \varphi}{\partial y}=0 \quad . \tag{4}$$

The density and dynamic viscosity of the liquid phase (water) and gas phase (air) are calculated by formulas:

The volume mass :

$$\rho=\varphi\rho_a+(1-\varphi)\rho_w \quad . \tag{5}$$

The dynamic viscosity:

$$\mu=\varphi\mu_a+(1-\varphi)\mu_w \quad . \tag{6}$$

Boundary conditions

A series of boundary conditions has been introduced to make the mathematical problem well established.

At $t = 0$:

- in water space: $[0, L] \times [0, h_w]$: $u = v = 0$, $\varphi = 0$.
- in air space: $[0, L] \times [h, H]$: $u = v = 0$, $\varphi = 1$.

At any time, $t > 0$, we have:

- outer boundaries ($x = 0$, $x = L$ at $y = 0$): $u = v = 0$.
- top external boundary ($y = H$): $p = 0$.

Darcy number is defined by:

$$\mathrm{Da}=\frac{K}{S} \quad . \tag{8}$$

No-slip conditions for the velocity was defined over all the walls remaining.

Nomenclature

u, v	velocity components (m^{-1})
x, y	space coordinates (m)
t	time (s)
g	gravitational acceleration (m s^{-1})
p	pressure (N m^{-2})
μ	dynamic viscosity (kg m^{-1} s^{-1})
μ_w	water dynamic viscosity (kg m^{-1} s^{-1})
μ_a	air dynamic viscosity (kg m^{-1} s^{-1})
ρ	density (kg m^{-3})
ρ_w	water density (kg m^{-3})
ρ_a	air density (kg m^{-3})
Da	Darcy number
k	porosity (m^2), K = DaS
S	surface
L	width of the framework
H	height of the framework
h_w	Height of the water

STATEMENT OF THE PROBLEM

Validation

This work, based on the experiment conducted by Liu, was validated with the improved SPH simulation of wave motions through porous media for Bing Ren et al. /16/ and the experimental data of Liu et al. /26/ at different time.

A comparison of the free surface of a fluid passing through a porous media in this numerical framework was made with those obtained by the improved SPH simulation of wave movements through porous media made by Bing Ren et al. /16/ and experimental data by Liu et al. /26/.

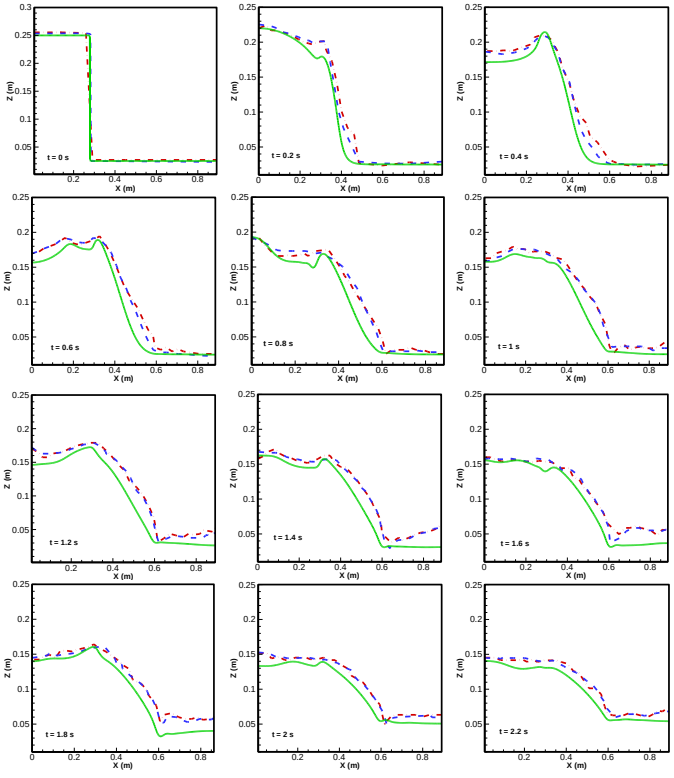

Figure 1. Comparison results of the water surface profile of a fluid through a porous medium (red dash dot: Liu et al. /26/, blue dash: SPH results by Bing et al. /16/, green solid: present study).

The obtained results for time from 0 to 2.2 s are presented in Fig. 1 and a good match of the water surface profile is achieved between the simulation and results presented by the two authors previously sited.

Methodology and set up

The objective is to study numerically the profile of the free surface of water, the pressure, and the pressure on the outer wall of the model, as well as the velocity field, using the dam-break wave passing through porous breakwater. The model is based on the experiment Liu et al. /26/ where a water rectangular tank was used.

The general geometry of the study is shown in Fig. 2, 0.37 m × 0.892 m; a multi porous structure of 0.29 m × 0.37 m was placed in the middle of the tank. The porous structure is composed of four different porous media with the same volume. The porosity of the four consecutive porous media is increasing from $Da_i = 10^{-6}$ to $Da_f = 10^{-3}$ in the first case and decreasing from $Da_i = 10^{-3}$ to $Da_f = 10^{-6}$ in the second, as presented in Fig. 3, where Da_i is the initial Darcy number designating the first porous media and Da_f is the final Darcy number designating the final porous media.

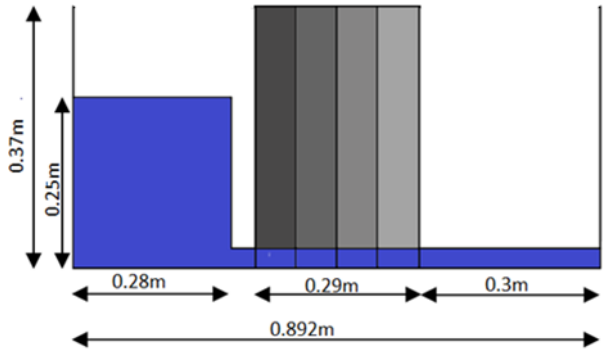

Figure2. General schematic setup of dam-break wave passing through different porous structures.

RESULTS AND DISCUSSION

The results of the numerical simulation are obtained for a solitary wave caused by dam failure, by studying the profile of the free surface, the velocity, as well as the effect of the pressure of the fluid spill and its impact on the external vertical wall, in the presence of a rectangular breakwater, provided with different consecutive porous media, in order to discuss and analyse the influence of such an arrangement.

The porous media composing the wave-breaker are placed in an increasing porosity and another time in a decreasing way, as shown in Fig. 3.

Figure 4 shows the water surface profile of a fluid passing through a breakwater composed of four different successive porous media. These media are placed from the smallest Da to the highest Da (from smallest porosity to the largest) and again in decreasing order, i.e., from highest Darcey to the smallest Darcey (from the largest porosity to the smallest).

Water starts to penetrate the first porous walls until 0.4 s where a large part of it is retained in the first wall of the smallest Da ($Da = 10^{-6}$) causing the wave to return to the dam and a small amount continues to pass through the other porous walls, but a large part of the wave is still retained in the dam before the porous breakwater. From 0.9 s the wave starts to return and replenish the breaker in the opposite direction thus decreasing the size of the hollow.

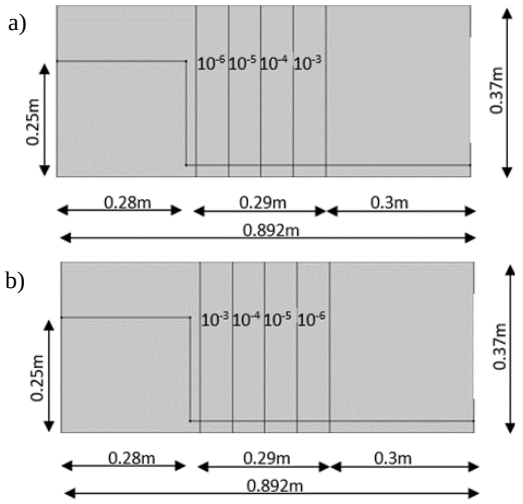

Figure 3. Configuration of the porous structure in the breakwater: a) porosity increasing; and b) porosity decreasing.

For the wave breaker with decreasing porosity, it is observed that it quickly penetrated the different porous layers compared to the previous case (wave breaker with increasing porosity). After 0.3 s, a return wave is created inside the breaker due to the very low porosity (permeability) of the last porous layer. At 0.6 s, the first wave arrives at the external wall and a narrow trough is formed. Return of the accumulated water in the wave breaker towards the dam is at 0.9 s, and at $t = 1$ s start of the return of the wave generated by water cumulated on the right side towards the external wall which repenetrates the wave breaker at 1.2 s tending to an equilibrium state.

A comparison of the pressure distribution of the fluid passing through the wave breaker of increasing and decreasing porosity is shown in Fig. 5. In both cases, the pressure is highest at the base (bed) of the dam. After a large part of the breaking wave has passed through the wave breaker with increasing Darcy number, the pressure at the bottom of the tank decreases.

As it is observed the pressure is very weak in the central panels where the porosity is equal to 10^{-5} and 10^{-4}, and high on both sides of the breaker.

After $t = 1.1$ s, the pressure is evenly distributed along the bed of the structure, where the volume of water is almost at the same height, thus reaching the first pressure balance. Whereas for the breakwater with decreasing Darcy number, the pressure is elevated in the lower part of the dam, between 0 and 0.2 s. While the breaking wave is blocked in the breaker because of the very low Darcy number of the last porous panel, the water is accumulating in the breaker leading to an increased pressure until $t = 0.7$ s. The pressure is distributed over the length of the framework, with a dip at the wave breaker just before the wave returns at $t = 1.1$ s, as the level of the wave decreases in the breaker (as a result of its passage to the right behind the wave breaker).

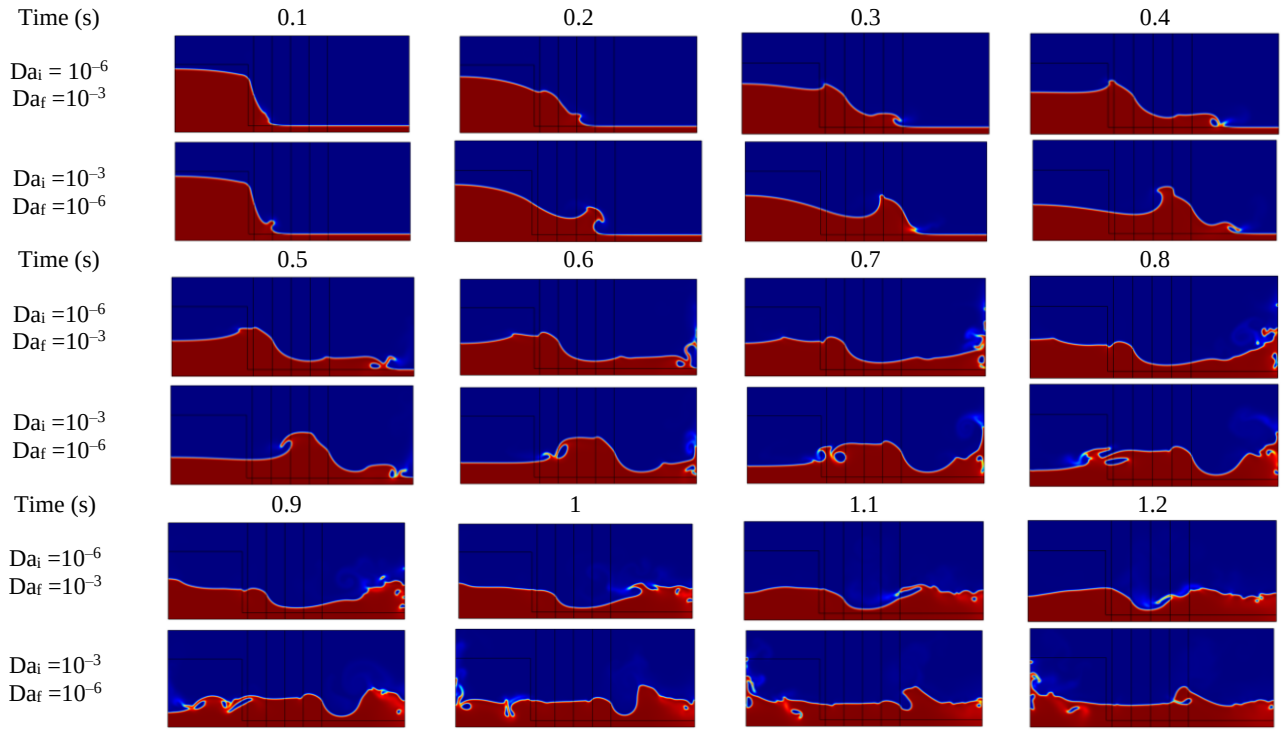

Figure 4. Comparison of the water surface profile of a fluid passing through different consecutive porous media with an increasing Darcy number ($Da_i = 10^{-6}$ to $Da_f = 10^{-3}$) and decreasing Darcy number ($Da_i = 10^{-3}$ to $Da_f = 10^{-6}$).

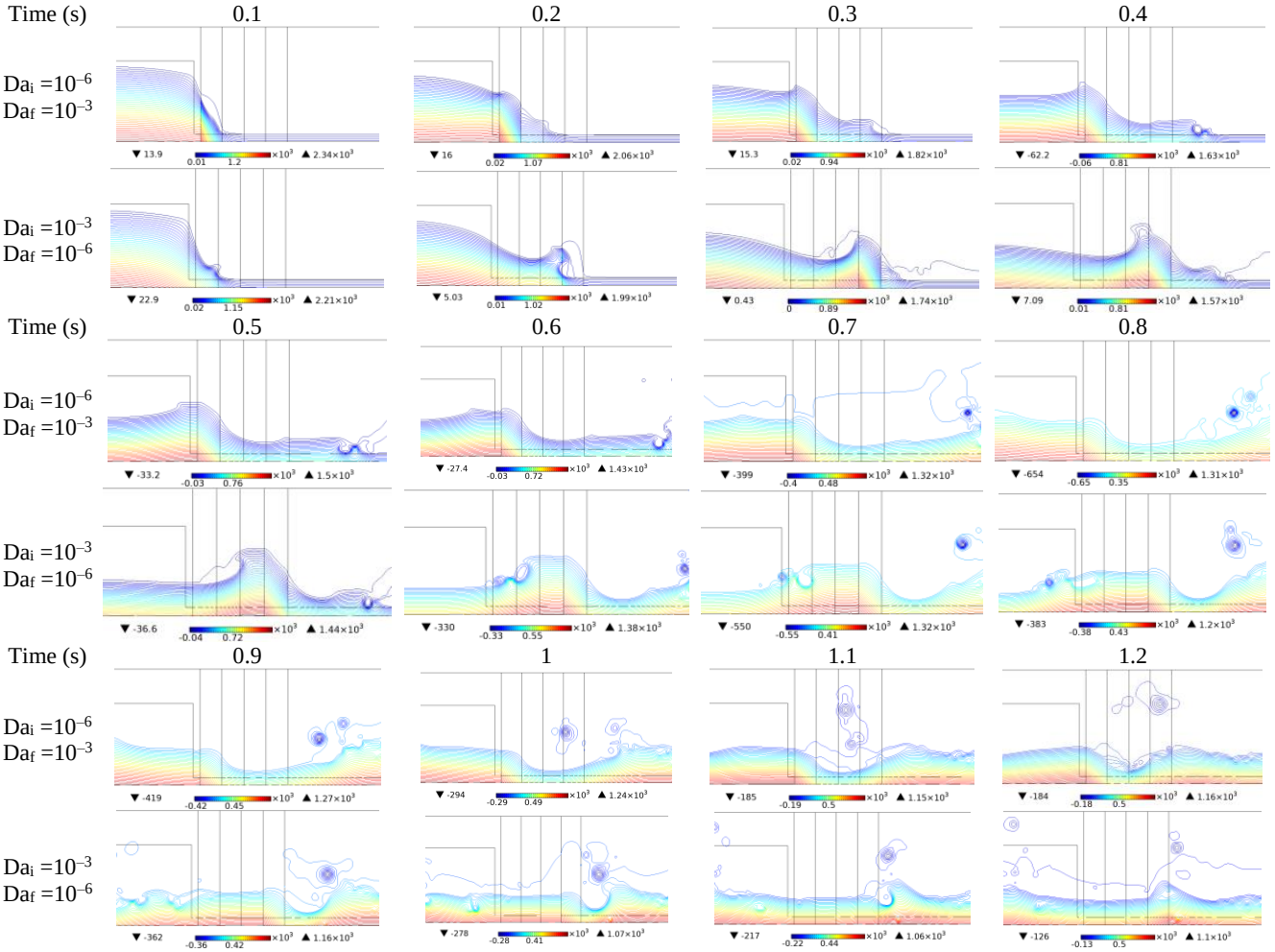

Figure 5. Comparison of the pressure distribution of fluid passing through a consecutive porous media with increasing Darcy number (Da = 10^{-6} to 10^{-3}) and decreasing Darcy number (Da = 10^{-3} to 10^{-6}).

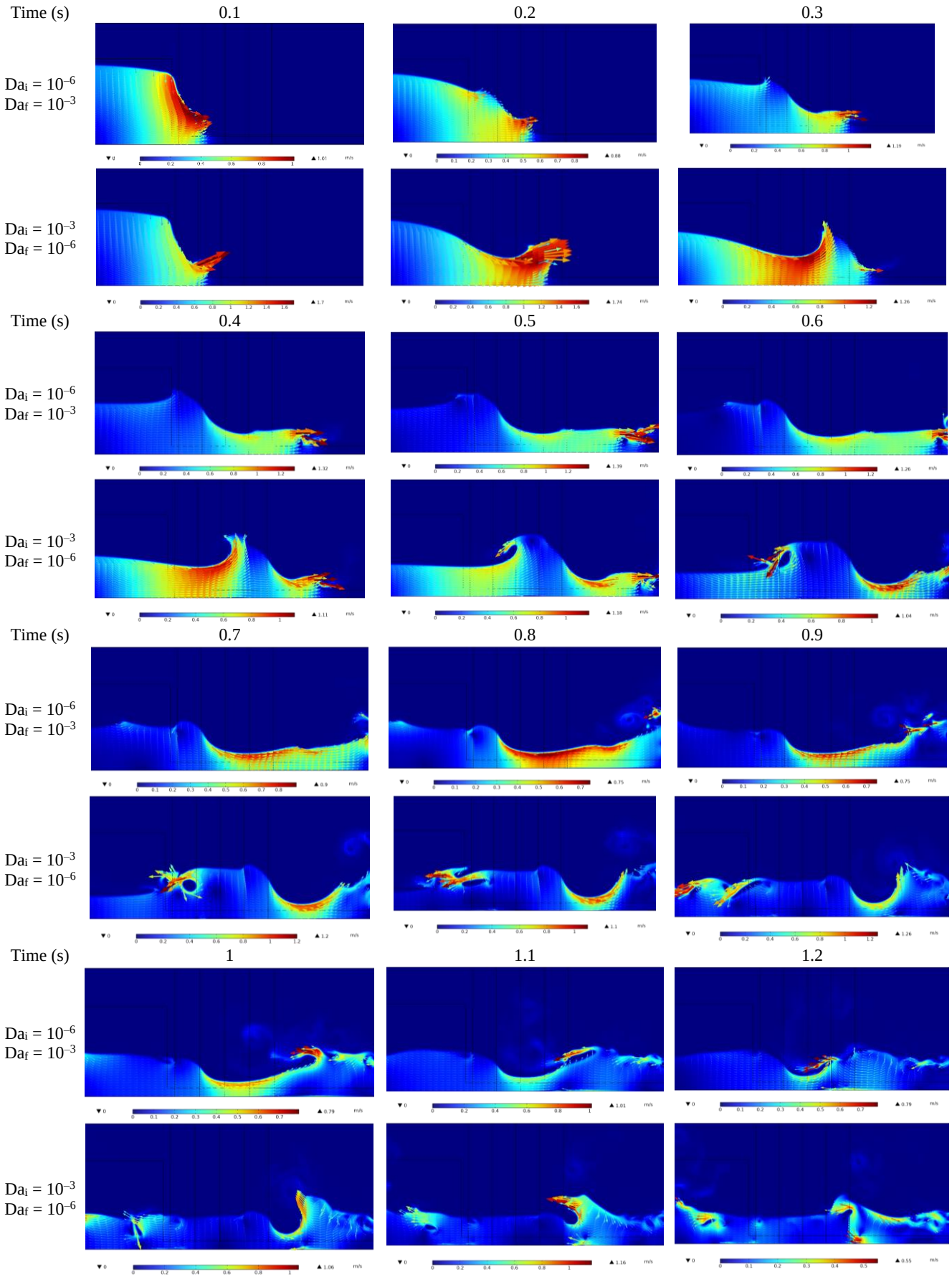

Figure 6. Comparison of the velocity field of fluid passing through a consecutive porous media with increasing Darcy number (Da =10^{-6} to 10^{-3}) and decreasing Darcy number (Da =10^{-3} to 10^{-6}).

The velocity profile of the breaking wave caused by dam failure is shown in Fig. 6. It can be seen that the wave advances at relatively uniform velocities at the beginning of the release because it is retained by the first wave breaker with Da = 10^{-6}. The velocities are higher at the lip as the wave advances, as it was noted that the maximal velocities are spread over the shoulder which feeds the return wave that takes shape at t = 1 s inside the wave breaker. For the second configuration where the porosity of the wave breaker is decreasing, it is observed that the wave not being retained reaches a maximal value at t = 0.2 s to be stopped in its momentum by the last panel with Da = 10^{-6}. The maximal velocities are reached during the splash of the wave. Following the analysis of Fig. 6, it is found that the velocities for the wave breaker configuration with decreasing porosity are mainly higher than the velocities for the wave breaker with increasing porosity.

The pressure on the external vertical wall caused by the breaking wave passing through the wave-breaker with decreasing porous medium is shown in Fig. 7. It is noted that the pressure is negative at t = 0.6 s for wave breaker with decreasing porous medium and at t = 0.5 and 0.6 s for wave-breaker with increasing porous medium, being the reason for decrease in flow rate translated by a depression caused by the presence of an air pocket in the wave-breaker.

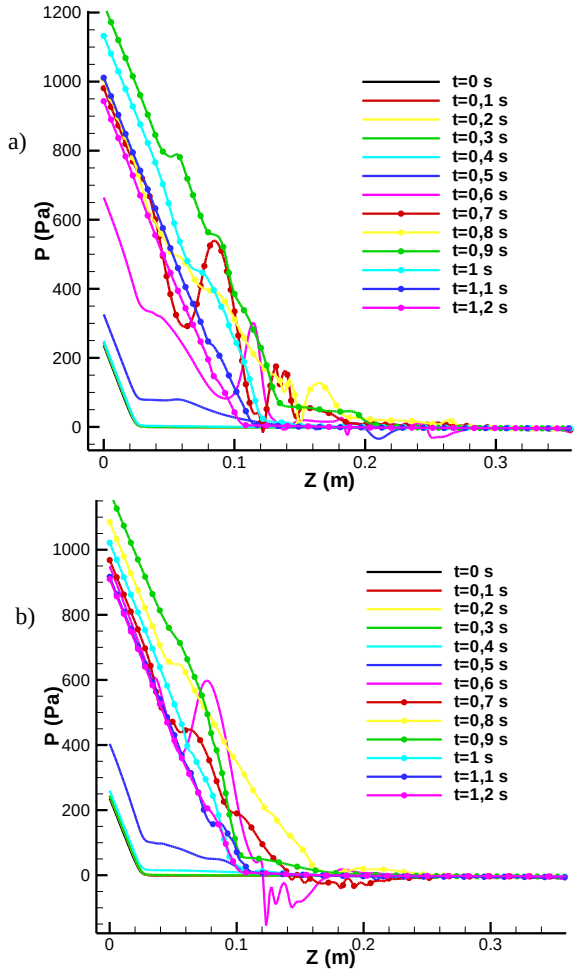

Figure 7. Pressure distribution comparison along external vertical wall through consecutive porous media with: a) increasing Da (Da = 10^{-6} to 10^{-3}); and b) decreasing Da (Da = 10^{-3} to 10^{-6}).

It is observed in both cases that the pressure is almost equal for the first instants (t = 0.1 to 0.4 s) because the wave still retained by the wave breaker had not yet reached the vertical wall. As it is observed that the pressure decreases and is almost zero beyond $z \approx 0.2$ m because the breaking wave never exceeds this height. The pressure is always very high in the lower part of the vertical wall where the water has accumulated. The pressure fluctuations shown in Fig. 7b at t = 0.7 and 0.8 s are a consequence of the variation in breaking wave force.

Pressures exerted by the breaking wave on the external vertical wall of the framework are more important in the case of the wave breaker provided with increasing porous medium.

CONCLUSION

Numerical results obtained for a breaking wave caused by a dam break passing through a porous medium rectangular wave breaker are presented in this paper. Equations are presented and solved numerically using the finite element method. Most important conclusions are:

- the wave passing through the wave breaker of decreasing porosity reaches the outer sidewall before the wave passing through the wave breaker of increasing porosity;
- the equilibrium state in the configuration where the breaker is fitted with panels with decreasing porosity is reached before the one fitted with panels with increasing porosity;
- in the case of the wave breaker provided with an increasingly porous medium, the pressures exerted by the breaking wave on the outer vertical wall of the frame are more important;
- the pressure exercised on the external side wall by the wave passing through the wave breaker fitted with panels of increasing porosity is stronger than that exercised on the one fitted with panels with decreasing porosity.

The current study presents several interesting results for the interaction of breaking waves with porous wave-breakers. These results can be used and extend the knowledge of wave breaking forces to the complex scenario of breaking wave interaction with porous structures.

REFERENCES

1. Peng, L., Zhang, T., Rong, Y., et al. (2021), *Numerical investigation of the impact of a dam-break induced flood on a structure*, Ocean Eng. 223: 108669. doi: 10.1016/j.oceaneng.2021.108669
2. Hu, K.C., Hsiao S.C., Hwung. H.H., Wu, T.R. (2012), *Three-dimensional numerical modeling of the interaction of dam-break waves and porous media*, Adv. Water Res. 47: 14-30. doi: 10.1016/j.advwatres.2012.06.007
3. Marsooli, R., Wu, W. (2014), *3-D finite-volume model of dam-break flow over uneven beds based on VOF method*, Adv. Water Res. 70: 104-117. doi: 10.1016/j.advwatres.2014.04.020
4. Issakhov, A., Borsikbayeva, A. (2021), *The impact of a multi-level protection column on the propagation of a water wave and pressure distribution during a dam break: Numerical simulation*, J Hydrol. 598(1-3): 126212. doi: 10.1016/j.jhydrol.2021.126212
5. Kamath, A., Chella, M.A., Bihs, H., Arntsen, Ø.A. (2016), *Breaking wave interaction with a vertical cylinder and the effect of breaker location*, Ocean Eng. 128: 105-115. doi: 10.1016/j.oceaneng.2016.10.025

6. Park, H., Do, T., Tomiczek, T., et al. (2018), *Numerical modeling of non-breaking, impulsive breaking, and broken wave interaction with elevated coastal structures: Laboratory validation and inter-model comparisons*, Ocean Eng. 158: 78-98. doi: 10.1016/j.oceaneng.2018.03.088
7. Sun, H., Sun, Z., Liamng, S. Zhao, X. (2019), *Numerical study of air compressibility effects in breaking wave impacts using a CIP-based model*, Ocean Eng. 174: 159-168. doi: 10.1016/j.oceaneng.2019.01.050
8. Kirkgöz, M.S. (1990), *An experimental investigation of a vertical wall response to breaking wave impact*, Ocean Eng. 17(4): 379-391. doi: 10.1016/0029-8018(90)90030-A
9. Kirkgöz, M.S. (1991), *Impact pressure of breaking waves on vertical and sloping walls*, Ocean Eng. 18(1-2): 45-59. doi: 10.1016/0029-8018(91)90033-M
10. Kirkgöz, M.S. (1992), *Influence of water depth on the breaking wave impact on vertical and sloping walls*, Coastal Eng. 18(3-4): 297-314. doi: 10.1016/0378-3839(92)90025-P
11. Kirkgöz, M.S. (1995), *Breaking wave impact on vertical and sloping coastal structures*, Ocean Eng. 22(1): 35-48. doi: 10.1016/0029-8018(93)E0006-E
12. Hattori, M., Arami, A., Yui, T. (1994), *Wave impact pressure on vertical walls under breaking waves of various types*, Coast. Eng. 22(1-2): 79-114. doi: 10.1016/0378-3839(94)90049-3
13. Manjula, R., Sannasiraj, S.A., Saravanan, S. (2015), *Experimental investigation of response of vertical slender cylinder under breaking wave impact*, Aquat. Procedia, 4: 227-233. doi: 10.1016/j.aqpro.2015.02.031
14. Sun, W.Y., Qu, K., Kraatz, S., et al. (2020), *Numerical investigation on performance of submerged porous breakwater to mitigate hydrodynamic loads of coastal bridge deck under solitary wave*, Ocean Eng. 213: 107660. doi: 10.1016/j.oceaneng.2020.107660
15. Zhao, E., Dong, Y., Tang, Y., Xia, X. (2021), *Performance of submerged semi-circular breakwater under solitary wave in consideration of porous media*, Ocean Eng. 223: 108573. doi: 10.1016/j.oceaneng.2021.108573
16. Ren, B., Wen, H., Dong, P., Wang, Y. (2016), *Improved SPH simulation of wave motions and turbulent flows through porous media*, Coast. Eng. 107: 14-27. doi: 10.1016/j.coastaleng.2015.10.004
17. Qiao, D., Feng, C., Yan, J., et al. (2020), *Numerical simulation and experimental analysis of wave interaction with a porous plate*, Ocean Eng. 218: 108106. doi: 10.1016/j.oceaneng.2020.108106
18. Koley, S., Panduranga, K., Almashan, N., et al. (2020), *Numerical and experimental modeling of water wave interaction with rubble mound offshore porous breakwaters*, Ocean Eng. 218: 108218. doi: 10.1016/j.oceaneng.2020.108218
19. Wu, W., Yang, Y., Zheng, H. (2020), *Hydro-mechanical simulation of the saturated and semi-saturated porous soil-rock mixtures using the numerical manifold method*, Comput. Methods Appl. Mech. Eng. 370: 113238. doi: 10.1016/j.cma.2020.113238
20. Wen, H., Ren, B., Wang, G. (2018), *3D SPH porous flow model for wave interaction with permeable structures*, Appl. Ocean Res. 75: 223-233. doi: 10.1016/j.apor.2018.04.003
21. Jafari, E., Namin, M.M., Badiei, P. (2021), *Numerical simulation of wave interaction with porous structures*, Appl. Ocean Res. 108: 102522. doi: 10.1016/j.apor.2020.102522
22. Hu, D., Li, F., Zhang, L., Zhang, K. (2020), *An advanced absorbing boundary for wave propagation analysis in saturated porous media*, Soil Dyn. Earthq. Eng. 136: 106204. doi: 10.1016/j.soildyn.2020.106204
23. Zhan, J.-M., Dong, Z., Han, Y., Jiang, W. (2010), *Numerical simulation of wave transformation incorporating porous media wave absorber*, J Hydrodyn. Ser. B, 22(5)Suppl.1: 982-985. doi: 10.1016/S1001-6058(10)60062-5
24. Carrillo, F.J., Bourg, I.C., Soulaine, C. (2020), *Multiphase flow modeling in multiscale porous media: An open-source micro-continuum approach*, J Comput. Phys.: X, 8: 100073. doi: 10.1016/j.jcpx.2020.100073
25. Grzybowski, H., Mosdorf, R. (2014), *Modelling of two-phase flow in a minichannel using level-set method*, J Physics: Conf. Ser. 530: 01204. doi: 10.1088/1742-6596/530/1/012049
26. Liu, P.L.-F., Lin, P., Chang, K.-A., Sakakiyama, T. (1999), *Numerical modeling of wave interaction with porous structures*, J Waterway, Port, Coastal, Ocean Eng. 125(6): 322–330. doi: 10.1061/(ASCE)0733-950X(1999)125:6(322)